Structural Basis of DNA Recognition and Mechanism of Quadruplex Formation by the β Subunit of the *Oxytricha* Telomere Binding Protein[†,‡]

Laurent Laporte and George J. Thomas, Jr.*

Division of Cell Biology and Biophysics, School of Biological Sciences, University of Missouri—Kansas City, Kansas City, Missouri 64110

Received September 29, 1997; Revised Manuscript Received November 24, 1997

ABSTRACT: Interactions of the β subunit of the *Oxytricha nova* telomere binding protein with the telomeric DNA sequences, $d(T_4G_4)_2$ and $dT_6(T_4G_4)_2$, have been investigated *in vitro* using Raman and fluorescence spectroscopies. Raman difference spectra show that the β subunit binds to both $d(T_4G_4)_2$ and $dT_6(T_4G_4)_2$ but promotes the formation of a parallel-stranded quadruplex only in $dT_6(T_4G_4)_2$, thus demonstrating the importance of the telomeric 5′ tail for *in vitro* recognition and guanine quadruplex formation. While $d(T_4G_4)_2$ is not a suitable substrate for quadruplex promotion by the β subunit, the Raman spectra reveal other structural rearrangements of this DNA strand upon β subunit binding, including changes in guanine glycosyl torsion angles from *syn* to *anti* and disruption of carbonyl hydrogen-bonding interactions. The conformation of $d(T_4G_4)_2$ in the β:$d(T_4G_4)_2$ complex is suggested as a plausible intermediate along the pathway to formation of the parallel-stranded guanine quadruplex. Fluorescence band shifts indicate that at least one of the two tryptophans of the β subunit is shielded from solvent as a consequence of DNA binding in both the β:$dT_6(T_4G_4)_2$ and β:$d(T_4G_4)_2$ complexes. However, the Raman spectra of these complexes suggest no significant changes in the β subunit secondary structure attendant with DNA binding. A model for β subunit binding by *Oxytricha* telomeric DNA sequences and a mechanism for quadruplex formation are proposed. A key feature of this model is the use of a telomeric hairpin secondary structure as the recognition motif.

Telomeres, the termini of eukaryotic chromosomes, ensure accuracy in genome replication and are essential for maintaining chromosome stability. They are characterized by a 5′ DNA strand that is rich in adenine and cytosine and a 3′ strand that is rich in thymine and guanine. Telomere loss is believed to lead to aberrant interchromosome fusion, incomplete or inaccurate replication, and cellular senescence (*1*−*4*). In most higher organisms, the telomere comprises both a double-stranded segment ranging from several bases to tens of kilobases and a single-stranded 3′ overhang. Although single stranded, the thymine/guanine-rich overhang is capable of forming higher order structures *in vitro* (*5*). In some organisms, the telomere is resistant to nuclease degradation, a characteristic that has been attributed to association with a specific telomere-binding protein (*6, 7*).

In the ciliated protozoan, *Oxytricha nova*, the 3′ telomeric strand consists of repeats of the sequence d(TTTTGGGG) or $d(T_4G_4)$, also referred to as Oxy1. Variants of this sequence have been investigated extensively using structural and biochemical methods. The results show that the *Oxytricha* telomeric repeat is capable of forming both intra- and intermolecular quadruplexes stabilized by Hoogsteen-bonded guanine quartets (*8*−*13*). Representative structures are shown in Figure 1. Quadruplex polymorphism is dependent upon a number of factors, including the type and concentration of cations present. For example, the parallel-stranded conformation of $d(T_4G_4)_4$ (Oxy4,[1] Figure 1C) is stabilized by high concentrations of K^+, while the antiparallel (foldback) conformation (Figure 1B) is stabilized by relatively low salt concentration (*12*).

Telomeres from *Oxytricha nova* (*14*) and other eukaryotes (*15, 16*) form specific nucleoprotein complexes in which a telomere-binding protein confers protection against nuclease digestion (*6, 7*). The *Oxytricha* telomere-binding protein is a heterodimer, comprising a 56-kDa α subunit and a highly basic 41-kDa β subunit (*17*). *In vitro* formation of the α:β:DNA ternary complex is cooperative (*18*). Because neither subunit alone binds strongly to telomeric quadruplexes, it has been proposed that nucleoprotein complex formation is mediated by single-strand recognition. In the absence of the α subunit, the β subunit promotes a dramatic increase (10^5-fold) in the rate of formation of guanine quadruplexes in single-stranded telomeric DNA (*18*). Despite this catalytic effect, it has been proposed that the β subunit functions as a chaperonin, navigating the DNA along a favorable pathway toward the formation of the telomeric quadruplex (*19*).

To further elucidate the role of the *Oxytricha* telomere-binding protein in quadruplex formation, we have investigated interactions of the α and β subunits with the telomeric sequences $d(T_4G_4)_2$ (Oxy2) and $dT_6(T_4G_4)_2$ (T6Oxy2). The preceding paper in this series (*20*) reported Raman spectro-

[†] Supported by NIH Grant GM54378.

[‡] Part LXVI in the series Raman Spectral Studies of Nucleic Acids.

* To whom correspondence may be addressed.

[1] Abbreviations: Oxy2, $d(T_4G_4)_2$; T6Oxy2, $dT_6(T_4G_4)_2$; Oxy4, $d(T_4G_4)_4$; β, 41-kDa subunit of the heterodimeric telomere binding protein of *Oxytricha nova*; dG, deoxyguanosine; dT, deoxythymidine.

S0006-2960(97)02400-8 CCC: $15.00
Published on Web 01/15/1998

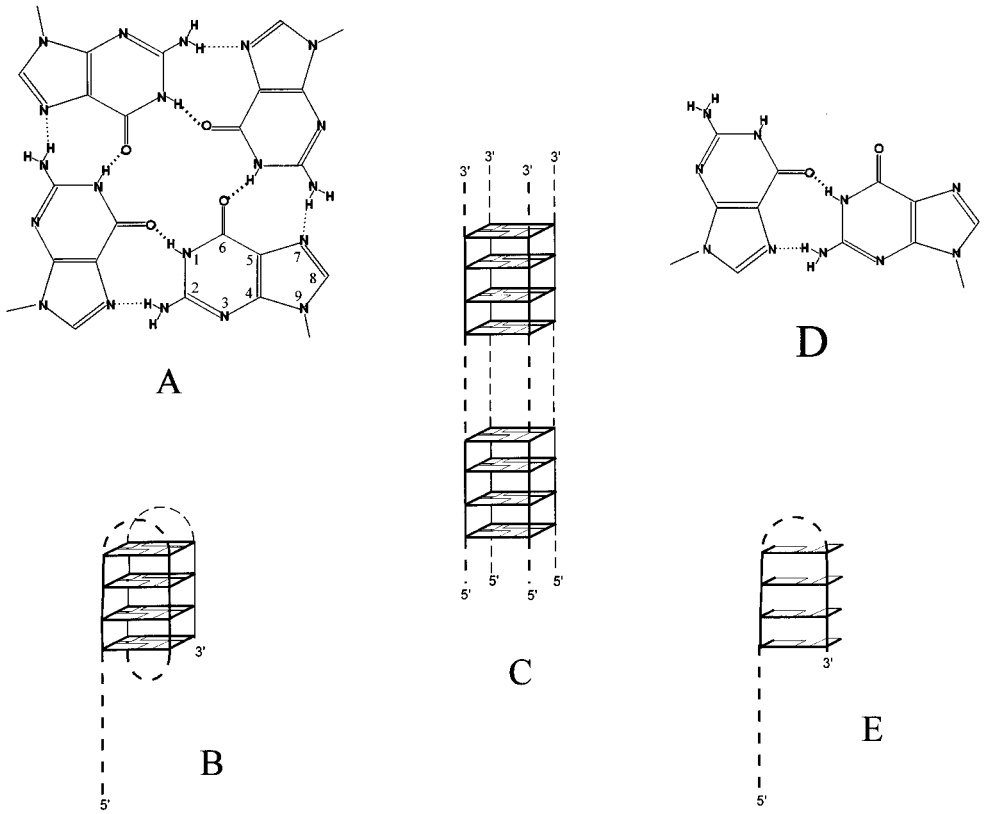

FIGURE 1: (A) Structure of a guanine quartet stabilized by Hoogsteen hydrogen bonds. (B) Representation of an antiparallel (foldback) quadruplex containing stacked guanine quartets and thymine tracts (dashed lines). In this structure, deoxyguanosine residues alternate between the C2′-*endo/syn* and C2′-*endo/anti* conformations. (C) Representation of a parallel (extended) quadruplex containing stacked guanine quartets and intervening thymine tracts. In this structure, all deoxyguanosines assume the C2′-*endo/anti* conformation. (D) Hoogsteen base pair proposed for the hairpin structures (E) of T6Oxy2 and Oxy2.

scopic signatures of both α and β subunits and examined the subunit thermostabilities and mutual interactions. The present paper focuses on DNA complexes of the β subunit. In the present analysis, Raman spectroscopy and fluorescence spectroscopy are utilized to probe the molecular basis of β subunit−DNA recognition and to identify structural changes induced in DNA with β subunit binding. The results indicate the nature of conformational changes in *Oxytricha* telomeric DNA and, importantly, demonstrate that the 5′ telomeric tail fulfills an important role in recognition. On the basis of the present findings, we propose a mechanism for β subunit binding and quadruplex formation in *Oxytricha* telomeric sequences.

MATERIALS AND METHODS

Subunit Preparation. The β subunit was expressed in *Escherichia coli* cells transformed by recombinant plasmid vectors, which were generously provided by Dr. Thomas R. Cech, University of Colorado. The protein was extracted from the cells and purified using procedures described previously (*18*−*20*). Samples were stored at −80 °C in a 50:50 volume percent mixture of glycerol and sample buffer (5 mM Tris, pH 7.5, containing 0.5 mM EDTA and 50 mM NaCl). Prior to spectroscopy, the protein was dialyzed extensively against sample buffer.

Oligonucleotide Preparation. Oligodeoxynucleotides $d(T_4G_4)_2$ (Oxy2; 4998 Da) and $dT_6(T_4G_4)_2$ (T6Oxy2; 6823 Da) were synthesized on an Applied Biosystems Model 381A DNA synthesizer and purified as described (*12*). Purified DNA was dissolved to 15 mg/mL with MilliQ water and adjusted to pH 7.2 ± 0.2 using either dilute HCl or NaOH. The final Na^+ concentration in these samples never exceeded 10 mM. Aliquots of the DNA solution were heated to 90 °C for 1.5 h, frozen immediately with liquid nitrogen, and lyophilized. Following lyophilization, each DNA was diluted to ≈30 mg/mL (4.4 mM for T6Oxy2 and 10 mM for Oxy2) with MilliQ water for spectroscopic investigation of the oligonucleotide solution conformation. Similarly, the DNA lyophilizate was dissolved in a 50 mg/mL (1.2 mM) stock solution of the β subunit for investigation of the β:DNA complex.

Complex Formation. Solutions of β ($\epsilon_{280} = 3.29 \times 10^4$ M^{-1} cm^{-1}) and Oxy2 ($\epsilon_{260} = 9.85 \times 10^3$ M^{-1} cm^{-1}) were mixed to achieve a 1:1 ratio and total concentration of 50 mg/mL at pH 7.3 ± 0.1. A similar procedure was followed for mixtures of β and T6Oxy2. Sodium concentrations were maintained below 90 mM. Samples were sealed in glass capillary tubes for Raman spectroscopy.

Raman Spectroscopy. Raman spectra were excited with the 514.5-nm line of an argon ion laser (Innova-70, Coherent Inc., Santa Clara, CA) using 200 mW of radiant power at the sample. The spectra were collected on a triple spectrograph (Triplemate Model 1877, SPEX Ind., Metuchen, NJ) equipped with a liquid nitrogen-cooled charge-coupled device detector (Model LN-CCD-1152UV, Princeton Instruments, Princeton, NJ) of 1152 × 298 pixels. The effective spectral slit width was approximately 5 cm^{-1}. Samples were maintained at 9 °C for all experiments by use of a thermostat

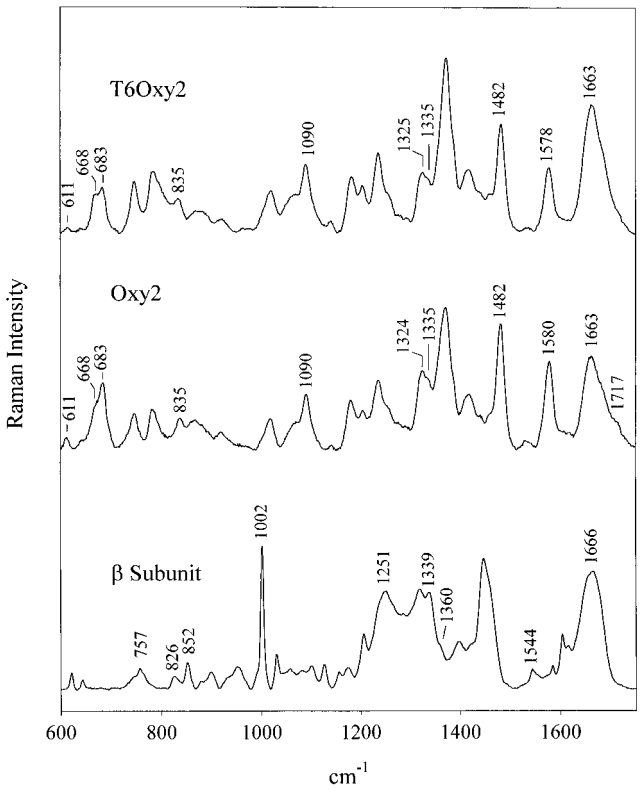

FIGURE 2: Raman spectra of T6Oxy2 (top), Oxy2 (middle), and the β subunit of the *Oxytricha nova* telomere binding protein (bottom) in H_2O solutions at pH 7.2 and 10 °C. Spectra were excited at 514.5 nm and corrected for solvent and baseline contributions.

designed for the 90° scattering geometry (*21*). Further details of the Raman instrumentation and sample illumination procedures have been described (*20, 21)*.

Fluorescence Spectroscopy. Fluorescence spectra of the β subunit, excited at 280 and 295 nm, and excitation spectra at 340 and 380 nm were collected on a Series 2 spectrofluorimeter (SLM/AMINCO, Urbana, IL) using a 4-nm slit width. Samples were dialyzed against 65 mM sodium phosphate buffer (pH 7.3), 0.5 mM EDTA, and 50 mM NaCl and were thermostated at 9 °C throughout experimental protocols. To eliminate protein absorption, solutions were serially diluted with sodium phosphate buffer until the observed change in fluorescence intensity was linear. The final protein concentration in these experiments was typically in the range of 500−700 nM, as determined by the absorbance at 280 nm.

Fluorescence spectra of β:DNA complexes were obtained similarly. Generally, a DNA stock solution was heated at 90 °C for 1.5 h to promote single-strand formation, and the solution was subsequently stored on ice. Complexes were prepared by adding aliquots (5−10 μL) of the DNA stock solution to the protein solution. Correction for the inner filter effect was carried out using standard procedures (*22*).

RESULTS AND INTERPRETATION

Raman Signature of the β Subunit. The Raman spectrum of the β subunit has been discussed previously (*20*). The solution spectrum in the 600−1750 cm^{-1} interval is reproduced in Figure 2 (lower trace) for comparison below with corresponding data obtained from complexes of the β subunit with DNA. Briefly, the amide I and amide III markers (*23*) identify a secondary structure that is rich in β-strand and irregular chain conformations but deficient in α-helix. The 13 tyrosine phenoxyls are on balance relatively strong hydrogen bond donors, as gauged from the diagnostic Fermi doublet intensity ratio ($I_{850}/I_{830} \approx 2.3$) (*24*). The orientations of subunit tryptophans, W93 and W343, are characterized by $|\chi^{2,1}|$ torsions of ∼80° and ∼100°, respectively (*20*).

Raman Signature of the Telomeric Repeat. Raman spectra in the 600−1750 cm^{-1} region of aqueous solutions of T6Oxy2 and Oxy2 are shown in Figure 2, upper and middle traces, respectively. Corresponding data (not shown) have also been obtained from D_2O solutions. Both T6Oxy2 and Oxy2 display Raman markers at 835 and 1090 cm^{-1} (*25, 26*), which are characteristic of phosphodiester linkages adopting the *gauche*$^-$/*gauche*$^-$ geometry. These Raman markers are similar to those reported previously for solution structures of Oxy4 (*27*).

Information regarding nucleoside sugar pucker and glycosyl orientations is contained in the complex band patterns of the 650−700 and 1300−1350 cm^{-1} intervals (*28*). For DNA of the canonical *B* form, i.e., containing only C2′-*endo*/*anti* nucleosides, definitive Raman markers are expected near 685 and 1333 cm^{-1} from dG residues in the C2′-*endo*/*anti* conformation. It is clear from Figure 2 that neither T6Oxy2 nor Oxy2 exhibits a simple 1333 cm^{-1} band diagnostic of C2′-*endo/anti*-dG. Instead, a Raman marker at 1325 cm^{-1} accompanies the 1333 cm^{-1} band, indicating the presence of both C2′-*endo/syn*-dG and C2′-*endo/anti*-dG (*27*). The intensity profile in the 650−700 cm^{-1} region of Figure 2 confirms that *syn*- and *anti*-dG conformers coexist in both T6Oxy2 and Oxy2. This is well illustrated in Figure 3, which shows the decomposition of the 650−700 cm^{-1} band envelope of deuterated T6Oxy2 and deuterated Oxy2. Here, deuteration is exploited to shift the otherwise interfering dT marker (*ca*. 668 cm^{-1}) to much lower frequency (653 cm^{-1}), thus revealing the distinctive C2′-*endo/syn*-dG marker at 677 cm^{-1} and C2′-*endo/anti*-dG marker at 685 cm^{-1}. [Neither of the dG markers is sensitive to deuteration (*27*).] Consistent results are obtained for H_2O solutions, as shown in Figure 3.

Information about guanine hydrogen bonding interactions in T6Oxy2 and Oxy2 is contained in the band near 1720 cm^{-1}, which involves carbonyl (C6═O) stretching, and in the band near 1482 cm^{-1}, which involves N7—C8 stretching (*12, 29*). The frequencies and intensities observed in Figure 2 are diagnostic of interbase hydrogen bonding by guanine C6═O and N7 acceptors (*12, 30*). Interbase hydrogen bonding is eliminated reversibly by heat denaturation and is replaced by solvent hydrogen bonding, which shifts the markers from 1482 and 1720 cm^{-1} to 1489 and 1685 cm^{-1}, respectively, in accordance with model compound results and previous telomeric DNA studies (*12, 27, 31*).

A weak band centered at 611 cm^{-1} is observed in spectra of both T6Oxy2 and Oxy2. We note that a similar band has been proposed elsewhere as a marker of the foldback antiparallel conformation of Oxy4, presumably originating from a preferred thymidine conformer within the T_4 loops (*12, 27*). The present results are consistent with the previous assignment to C2′-*endo/syn*-dT and suggest a similar dT conformation in loops of the foldback quadruplex and hairpin.

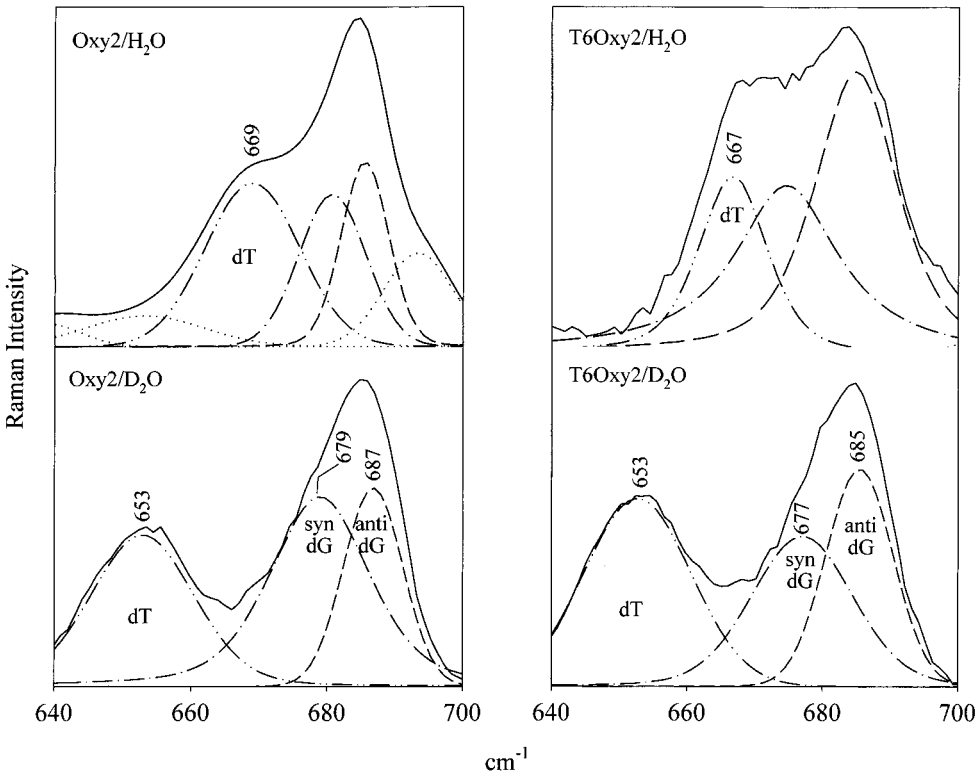

FIGURE 3: Raman spectral profiles of Oxy2 (left panel) and T6Oxy2 (right panel) in the 640−700 cm^{-1} region. The D_2O solution spectra (bottom) provide the basis for a curve-fitting assessment of dG conformations in Oxy2 and T6Oxy2, as indicated by the labeled Raman markers. The H_2O solution spectra (top) establish hydrogen-isotope shifts diagnostic of the principal dT marker, as labeled. (See further discussion in text.) In the curve-fitting analysis, a minimum of two components was required to satisfactorily fit the broad and asymmetric dG band near 685 cm^{-1}. Models with one component produced a poor fit, as gauged by the residuals and reduced χ^2 values, while models utilizing more than two components did not improve the fit significantly. [Unassigned bands near 640 and 695 cm^{-1} in H_2O solution spectra, indicated by the dotted curves, are not included in the present analysis and are discussed by Miura and Thomas (*27*).]

Hydrogen → deuterium exchange experiments suggest that both Oxy2 and T6Oxy2 adopt a secondary structure in which both *syn* and *anti* conformations of deoxyguanosine are present (data not shown), consistent with results obtained in H_2O solvent. Upon influx of D_2O, we observe virtually instantaneous exchange for half of the guanine imino protons and exchange kinetics for the remaining half, with rates of 4.6×10^{-3} min^{-1} for Oxy2 and 9.6×10^{-3} min^{-1} for T6Oxy2 (data not shown). An inhibition in proton exchange for half of the guanine imino protons is consistent with the formation of a hairpin structure that is stabilized by Hoogsteen G·G base pairs. Results from native gel electrophoresis are consistent with the conclusion from the Raman of a compact DNA structure. Both T6Oxy2 and Oxy2 exhibit enhanced electrophoretic mobility relative to their isomers $dT_6(TG)_8$ and $d(TG)_8$, consistent with the formation of hairpins (data not shown).

In summary, the Raman spectrum of T6Oxy2, like that of Oxy2, indicates an ordered secondary structure containing the *gauche*$^-$/*gauche*$^-$ phosphodiester conformation, both *syn* and *anti* conformations of deoxyguanosine and Hoogsteen G·G pairing. Hydrogen → deuterium exchange experiments are consistent with the presence of Hoogsteen G·G pairing and both *syn* and *anti* conformations of deoxyguanosine, while native gel electrophoresis indicates that the telomere strands form compact structures. Consistent with these structural features is the formation of a "hairpin" by the GGGGTTTTGGGG sequence of each oligomer.

Structure Polymorphism of T6Oxy2 and Oxy2. Both T6Oxy2 and Oxy2 exhibit salt-dependent polymorphism, similar to that reported previously for the Oxy4 sequence (*27*, *32*). Figure 4 shows the Raman signatures of T6Oxy2 in ~10 mM Na^+ and 150 mM K^+, in the upper and middle traces, respectively. The Raman signatures as well as gel mobility and hydrogen/deuterium exchange studies (*31*) demonstrate that the corresponding secondary structures are a foldback antiparallel duplex (hairpin) and an extended parallel-stranded quadruplex. The difference spectrum of Figure 4 (upper trace minus lower trace) reveals the Raman spectral changes attendant with this transformation of T6Oxy2 from hairpin to quadruplex.

The difference spectrum of Figure 4 bears a remarkably close correspondence to spectral changes accompanying the conversion of Oxy4 from a foldback antiparallel quadruplex to an extended parallel-stranded quadruplex (*27*). Noteworthy are the 675 → 685 and 1325 → 1336 cm^{-1} shifts of key dG markers, indicating the conversion of C2′-*endo*/*syn*-dG to C2′-*endo*/*anti*-dG. Difference features in the 730−820 cm^{-1} interval (dT and backbone markers, Figure 4) also resemble those observed for the Oxy4 transformation (*27*). It is clear from the present and previous results that the Raman signatures of the hairpin (T6Oxy2) and foldback quadruplex (Oxy4) exhibit many similarities. Nevertheless, these Raman fingerprints are not identical. The most important difference between these two low-salt structures is their different requirements for Hoogsteen hydrogen bonding. The hairpin requires one N7 acceptor per G·G base pair, while the quadruplex requires four per quartet (cf. Figure 1A,D). As expected (*29*, *30*, *33*, *34*), this difference in guanine hydrogen bonding is revealed by Raman markers

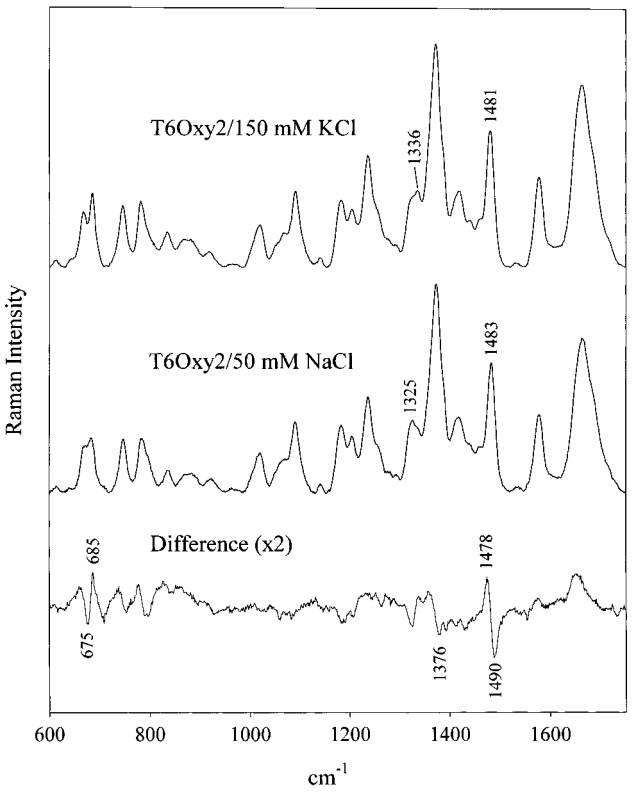

FIGURE 4: Raman spectra of T6Oxy2 in the parallel quadruplex conformation (150 mM KCl; top trace) and hairpin conformation (50 mM NaCl; middle trace) and their difference spectrum (bottom trace; amplified 2-fold). Other experimental conditions are given in the Figure 2 legend.

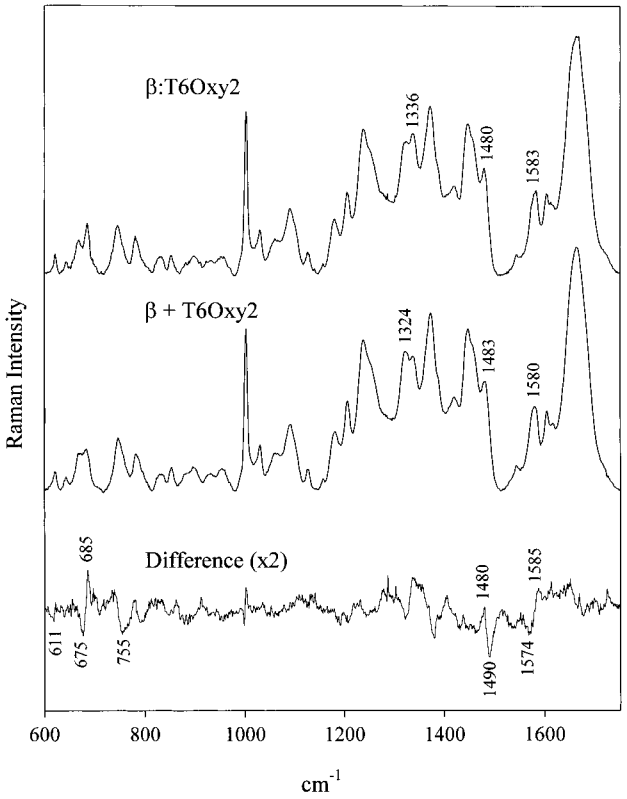

FIGURE 5: Raman spectra of the β:T6Oxy2 complex (top), sum of constituents (middle), and their difference spectrum (amplified 1.5-fold). Other experimental conditions are given in the Figure 2 legend.

near 1480−1490 cm^{-1} (Figure 4). Thus, for T6Oxy2, the dG marker exhibits a significant displacement of intensity from 1490 to 1478 cm^{-1} upon conversion from hairpin to quadruplex (Figure 4), whereas in Oxy4, no similar spectral change occurs (*27*). An analysis of structural polymorphism in T6Oxy2 and Oxy2 and a more detailed comparison with Oxy4 will be reported elsewhere (*31*).

Complex of the β Subunit with T6Oxy2. Figure 5 compares the Raman spectrum of the β:T6Oxy2 complex (upper trace) with the spectral sum of constituents (middle trace). Major differences are apparent in DNA marker bands at 685, 742, 1336, and 1480 cm^{-1}. The computed difference spectrum (lower trace = upper trace − middle trace) shows that a number of other changes also occur in DNA band frequencies and/or intensities attendant with complex formation. Thus, binding of the β subunit induces a dramatic structural change in T6Oxy2. The nature of this structural change is revealed by comparison of Figure 5 (lower trace) with the difference spectrum that corresponds to the salt-induced structure transformation of T6Oxy2 from hairpin to quadruplex (Figure 4, lower trace).

The principal difference features in the lower trace of Figure 5 may be interpreted by analogy with the data shown in the lower trace of Figure 4 and previously investigated telomeric DNA sequences (*27*). For example, the 675 → 685 and 1324 → 1336 cm^{-1} shifts reflect the C2′-*endo/syn*-dG → C2′-*endo/anti*-dG conformation change, while the intensity increase at 1376 cm^{-1} reflects a change in environment of thymine C5H$_3$ groups (*33*, *34*). The 730−820 cm^{-1} region also exhibits a difference band pattern similar to that observed for T6Oxy2, attributable to changes in dT conformation from C2′-*endo*/*syn* to C3′-*endo*/*anti* (*35*).

Although the lower traces of Figures 4 and 5 are generally similar, a significant dissimilarity is apparent at 755 cm^{-1}. The 755 cm^{-1} difference band in β:T6Oxy2 (Figure 5, lower trace) is much more intense than its counterpart shown in the lower trace of Figure 4. This can be attributed to contributions from subunit tryptophans in the complex. Sensitivity of the tryptophan marker band near 757 cm^{-1} to indole ring environment has been noted by Takeuchi and Harada (*36*) and Miura *et al*. (*37*). Further evidence of a net change in environment of β subunit tryptophans upon telomeric DNA binding is provided by fluorescence spectroscopy (see Fluorescence Spectroscopy). The lower trace in Figure 5 also exhibits for β:T6Oxy2 a guanine band shift (1574 → 1585 cm^{-1}) that has no counterpart in T6Oxy2 (Figure 4, lower trace). This can be attributed to different interactions of guanine exocyclic amino groups in the two cases (*31*).

Complex of the β Subunit with Oxy2. Figure 6 compares Raman spectra of β:Oxy2 and its constituents. As in the case of the β:T6Oxy2 complex (above), subunit binding causes major changes in Oxy2 marker bands, indicating altered DNA structure. However, the spectral changes observed here differ qualitatively from those noted above (*cf*. lower traces of Figures 5 and 6) and include additional perturbations to protein marker bands. For example, difference features at 829 and 851 cm^{-1} are consistent with altered hydrogen bonding of subunit tyrosines (*24*). The change observed in the tyrosine Fermi doublet intensity ratio, I_{851}/I_{829}, suggests a change in hydrogen bonding of the average

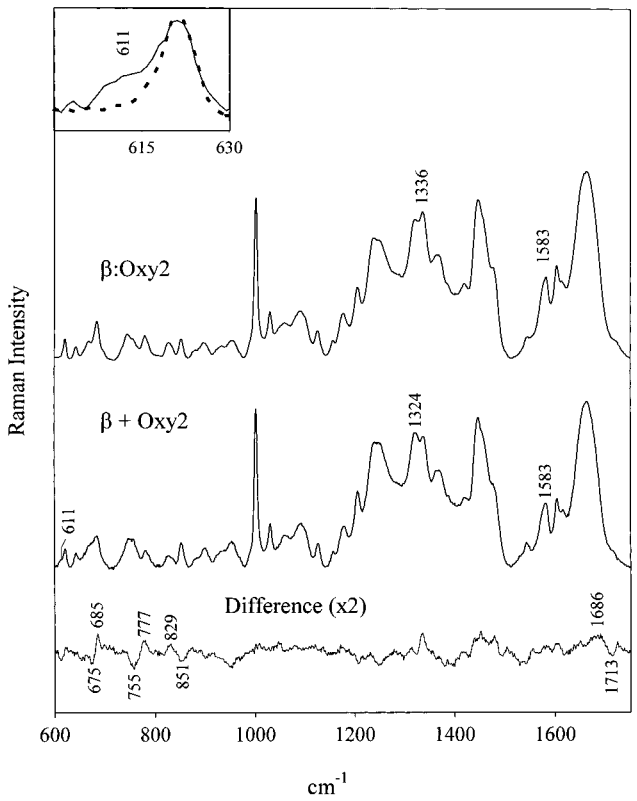

FIGURE 6: Raman spectra of the β:Oxy2 complex (top), sum of constituents (middle), and their difference spectrum (amplified 1.5-fold). The inset at the upper left compares the 600−630 cm^{-1} region of the complex (broken line) and sum of constituents (solid line) on an expanded scale to illustrate the absence of the 611 cm^{-1} dT marker in the complex. Other experimental conditions are given in the Figure 2 legend.

phenoxyl from strong acceptor in the unbound protein ($I_{851}/I_{829} = 2.4$) to moderate donor/acceptor in the bound protein ($I_{851}/I_{829} = 1.3$).

With respect to DNA markers, the guanine band at 1713 cm^{-1} is shifted to 1686 cm^{-1} in β:Oxy2 but not in β:T6Oxy2. Because the 1713 cm^{-1} band shifts to lower frequency with disruption of G·G pairing (*12*, *31*) and is due to a vibrational mode involving 6C═O stretching and N1−H in-plane bending (*29*), the observed shift signifies disruption of base pairing in the Oxy2 hairpin by β subunit binding. Conversely, the β:Oxy2 difference spectrum lacks the definitive band shifts (1490 → 1480 and 1574 → 1585 cm^{-1}) observed for β:T6Oxy2. The absence of such shifts indicates no net change in hydrogen bonding of guanine N7 or NH_2 groups. Accordingly, the structural interpretation given above for β:T6Oxy2 does not apply to β:Oxy2. Instead it appears that interbase hydrogen bonds of the protein-free Oxy2 hairpin are replaced by comparable protein−DNA hydrogen bonds in β:Oxy2.

Although β:T6Oxy2 and β:Oxy2 difference spectra are dissimilar overall, they share certain key features. For example, shifts of Raman markers diagnostic of dG conformational change (675 → 685 and 1324 → 1336 cm^{-1}) are striking. These indicate that *syn*-dG conformers present in Oxy2 are eliminated in β:Oxy2.

We note two other key characteristics of the Raman spectrum of β:Oxy2 (Figure 6, upper trace and inset) that are common also to β:T6Oxy2 (Figure 5, upper trace). These are (i) the elimination of the weak band at 611 cm^{-1}, a C2′-*endo/syn*-dT marker (*12*), and (ii) an accompanying enhancement of the band at 777 cm^{-1}, a C3′-*endo/anti*-dT marker (*35*). These features are clearly more apparent in β:Oxy2, which we attribute to their origin in the thymine hairpin loop.

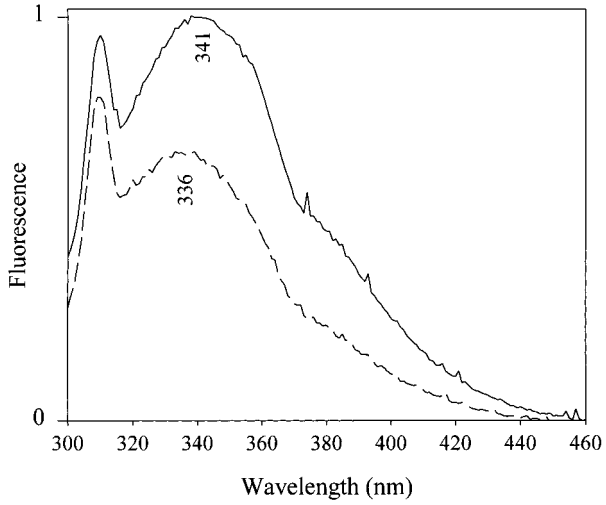

FIGURE 7: Fluorescence spectra of the β:T6Oxy2 complex (broken line) and isolated β subunit (solid line), each excited at 280 nm. The sharp peak near 310 nm is due to Raman scattering of H_2O.

Fluorescence Spectroscopy. The fluorescence spectrum of β:T6Oxy2 excited at 280 nm is shown in Figure 7. Similar spectra were obtained for β:Oxy2. Excitation at 295 nm (data not shown) produces virtually identical results. Thus, the observed emission is attributed only to the two tryptophan residues of the β subunit. For both β:Oxy2 and β:T6Oxy2, DNA binding shifts the wavelength maximum of tryptophan emission from 341 to 336 nm, and the band intensity is quenched by about 30%. The fluorescence quenching is typical of DNA−protein complexes, and the observed blue shift is indicative of a net decrease in polarity of the average indole environment (*22*, *38*). The fluorescence results are therefore consistent with the Raman results in demonstrating that the net tryptophan environment is more hydrophobic in the complex than in the free protein. This may result from shielding of either one or both tryptophans by DNA.

DISCUSSION AND CONCLUSIONS

The β Subunit Promotes Quadruplex Formation in T6Oxy2. In the absence of the β subunit, the secondary structure formed by T6Oxy2 is a hairpin stabilized by G·G pairs and requiring both C2′-*endo/syn*- and C2′-*endo/anti*-dG conformers. Additional details of this structure are revealed by hydrogen/deuterium exchange kinetics, which will be reported elsewhere (*31*). The present study shows that the hairpin structure of T6Oxy2 is converted by the β subunit to a four-stranded structure containing guanine quartets that exhibit only the C2′-*endo/anti*-dG conformation. The Raman markers signaling the hairpin to quadruplex transformation are identical with those indicative of quadruplex formation in Oxy4 upon heating in the presence of K^+ ions (*12*, *27*). The spectroscopic results are supported by native gel electrophoresis, which reveals the formation of a low mobility structure for T6Oxy2 following β subunit interaction (data not shown). A similar conclusion has been reached by Fang and Cech (*19*), who investigated the effect of

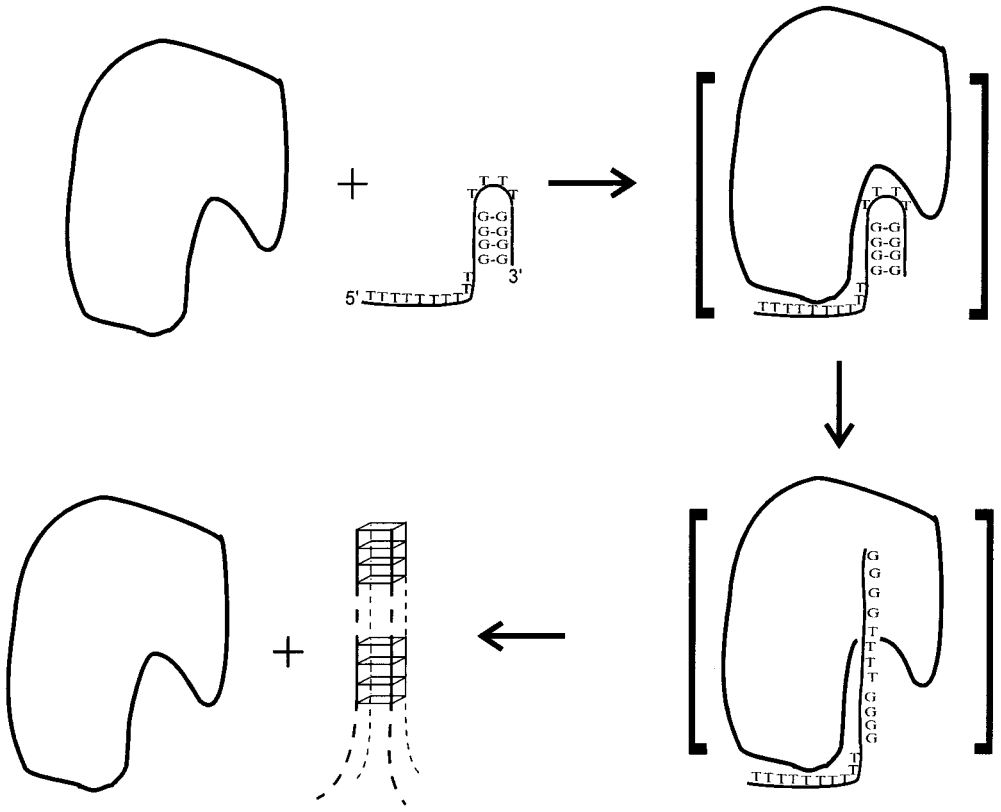

FIGURE 8: Schematic representation of the hairpin to quadruplex transformation induced in the *Oxytricha* telomeric DNA repeat (T6Oxy2) by the β subunit of the telomere binding protein. In this model, a telomeric hairpin is proposed as the DNA recognition motif for the β subunit. The telomeric hairpin is stabilized by G·G base pairs and contains both *syn* and *anti* dG conformers. Although the stoichiometry of the DNA−protein complex is undetermined, a 1:1 stoichiometry is assumed for simplicity. Upon binding, G·G pairs are ruptured, and the hairpin is destabilized in favor of a single strand containing only *anti* dG conformers. Telomeric single strands subsequently associate to form the extended parallel quadruplex, which is stabilized by hydrogen-bonded guanine quartets (parallelogram symbols) separated by runs of thymines (dashed lines).

β subunit binding on other DNA oligomers containing the dT_4G_4 repeat. The β-induced structure transformation of T6Oxy2 is represented schematically in Figure 8.

The present results suggest additional details of the hairpin to quadruplex transformation of T6Oxy2. The intensity of the thymine Raman marker at 1376 cm^{-1} indicates a more hydrophilic environment for thymine methyl groups in the quadruplex than in the hairpin, presumably due to more extensive interactions with aqueous solvent in the former (*33*, *34*). This implies a rearrangement of thymines in the quadruplex, where packing of T_4-spaced guanine quartets could lead to bulging of the intervening T_4 segments and increased solvation of thymine rings. A similar juxtaposition of guanine quartets occurs between neighboring quadruplexes in the crystal structure of d(TGGGGT), with attendant exposure of thymines to the hydrophilic solvent (*10*). On the other hand, Gupta and co-workers (*39*) have found a completely different arrangement of thymines in the crystal structure of the parallel-stranded dT_4G_4 quadruplex. In dT_4G_4, the thymine methyl groups are directed toward the 4-fold axis, where they are relatively inaccessible to solvent.

The present study also provides some insight into the molecular mechanism of β subunit binding to T6Oxy2. Observed fluorescence and Raman band shifts imply a net increase in the hydrophobicity of subunit tryptophan environments with binding. Assuming the formation of a stable β:T6Oxy2 complex, the spectral shifts reflect interaction of tryptophans either directly with DNA or indirectly with other side chains affected by DNA binding.

The β Subunit Does Not Promote Quadruplex Formation in Oxy2. In the absence of the β subunit, the secondary structure formed by Oxy2, like that of T6Oxy2, is a hairpin stabilized by G·G pairs consisting of both *syn*- and *anti*-dG conformers. The β subunit induces a structural transformation of the Oxy2 hairpin, although the product is *not* a quadruplex. DNA structure in the β:Oxy2 complex is distinguished by the absence of G quartets as well as by the loss of G·G pairs and *syn*-dG conformers. In addition, to its C2′-*endo/anti*-dG conformers, the transformed Oxy2 structure is characterized by a predominance of *anti*-dT conformers. We propose a single strand as the likely chain conformation.

The tertiary structure of β is altered significantly by Oxy2 binding, as evidenced by major changes in tyrosine environments. Because the vast majority of tyrosines (11 of 13) are located within the amino-terminal 140 residues, it is suggested that this domain plays a key role in Oxy2 recognition. As with β:T6Oxy2, we find in β:Oxy2 that the average tryptophan environment is also sensitive to DNA binding.

Mechanism of Telomeric Quadruplex Formation. Both T6Oxy2 and Oxy2 assume similar hairpin secondary structures and both interact with the β subunit, demonstrating a common DNA recognition domain in the protein. However, the two sequences respond differently to this interaction. T6Oxy2 is converted to a quadruplex; Oxy2 is not. The basis for this difference in structural response apparently resides

in the 5′ telomeric tail and demonstrates a second aspect of the recognition domain.

The present results are consistent with the following mechanism of β-induced quadruplex formation in T6Oxy2. The telomeric DNA hairpin containing *syn*- and *anti*-dG conformers is recognized and bound by the β subunit, forming a complex of as yet unspecified stoichiometry (*18*). Once bound, the telomeric hairpin structure is destabilized in favor of a parallel-stranded quadruplex, which presumably requires protein-mediated disruption of the hairpin G·G base pairs, formation of an extended single strand with only *anti*-dG conformers, and subsequent strand associations. The 5′ telomeric tail may remain bound to the β subunit during interstrand association or may exploit another means of ensuring guanine quartet formation. While the present studies have been focused (for spectroscopic simplicity) on a homothymidine tail, other studies suggest that the specific base sequence within the 5′ tail is not a determining factor in quadruplex formation (*18, 19*).

Similar initial steps are proposed for the mechanism of β subunit binding and hairpin destabilization of telomeric DNA lacking a 5′ tail. However, once G·G base pairs are disrupted in this DNA substrate, the β subunit does not mediate quadruplex formation. This could be due to a particular stoichiometry of the complex or to a key structural constraint imposed by the absence of the 5′ nucleotides. We favor the latter explanation and speculate that the β subunit requires a DNA binding domain significantly greater than four nucleotides in length. In the absence of such a tail, we envision the protein as binding beyond the initial 5′-T_4 sequence and preventing quartet formation in the adjoining guanines of the first Oxy repeat. This may be sufficient to block extended quadruplex formation. Because the β:Oxy2 complex does not proceed to the formation of stable telomeric quadruplexes, it may be regarded as an "intermediate" along the pathway to productive quadruplex formation.

In summary, Raman spectra of the β:Oxy2 and β:T6Oxy2 complexes provide new insight into the mechanism of quadruplex formation promoted by the β subunit. In particular, the present results suggest that a DNA hairpin secondary structure containing G·G base pairs is required for β subunit binding. While the hairpin is necessary for β subunit binding, it is not sufficient for quadruplex formation. When the hairpin lacks a 5′ tail, as in the case of Oxy2, binding to the β subunit and disruption of the hairpin conformation still occur but do not lead to formation of the quadruplex.

Because the *Oxytricha* α and β subunits form a heterodimer only in the presence of DNA, free α subunits and/or free β subunits are likely to occur in the nucleus. The results presented here leave open the possibility that free β subunits may be required to unfold naturally occurring hairpin structures so that the productive α:β:DNA ternary complex can be formed. This question will be further addressed in a forthcoming study of interactions of the α subunit that lead to formation of binary and ternary complexes (L. Laporte and G. J. Thomas, Jr., manuscript in preparation).

ACKNOWLEDGMENT

We thank Professor Thomas R. Cech of the University of Colorado, Boulder, who generously provided plasmids and cells for expression of the *Oxytricha* telomere binding proteins. We also thank Dr. James M. Benevides for assistance in many phases of this work.

REFERENCES

1. Blackburn, E. H. (1994) *Cell 77*, 621−623.
2. Blackburn, E. H., and Greider, C. W., Eds. (1995) *The Telomeres*, CSHL Press, Cold Spring Harbor, New York.
3. Lundblad, V., and Szostak, J. W. (1989) *Cell 57*, 633−643.
4. Sandell, L. L., and Zakian, V. A. (1993) *Cell 75*, 729−739.
5. Sen, D., and Gilbert, W. (1990) *Nature 344*, 410−414.
6. Price, C. M., and Cech, T. R. (1987) *Gen. Dev.* 783−793.
7. Raghuraman, M. K., and Cech, T. R. (1989) *Cell 59*, 719−728.
8. Smith, F. W., and Feigon, J. (1993) *Biochemistry 32*, 8682−8692.
9. Wang, Y., and Patel, D. (1995) *J. Mol. Biol. 251*, 76−94.
10. Laughlin, G., Murchie, A. I. H., Norman, D. G., Moore, M. H., Moody, P. C. E., Lilley, D. M. J., and Luisi, B. (1994) *Science 356*, 520−524.
11. Kang, C. H., Zhang, X., Ratliff, R., Moyzis, R., and Rich, A. (1992) *Nature 356*, 126−131.
12. Miura, T., and Thomas, G. J., Jr. (1995) *Biochemistry 34*, 9645−9654.
13. Raghuraman, M. K., and Cech, T. R. (1990) *Nucleic Acids Res. 18*, 4543−4552.
14. Price, C. M., and Cech, T. R. (1989) *Biochemistry 28*, 769−774.
15. Price, C. M., Skopp, R., Krueger, J., and Williams, D. (1992) *Biochemistry 31*, 10835−10843.
16. Zhong, Z., Shiue, L., Kaplan, S., and de Lange, T. (1992) *Mol. Cell. Biol. 12*, 4834−4843.
17. Fang, G., and Cech, T. R. (1993) *Proc. Natl. Acad. Sci. U.S.A. 90*, 6056−6060.
18. Fang, G., and Cech, T. R. (1993) *Biochemistry 32*, 11646−11657.
19. Fang, G., and Cech, T. R. (1993) *Cell 74*, 875−885.
20. Laporte, L., Stultz, J., and Thomas, G. J, Jr. (1997) *Biochemistry 36*, 8053−8059.
21. Thomas, G. J., Jr., and Barylski, J. R. (1970) *Appl. Spectrosc. 24*, 463−464.
22. Lakowicz, J. R. (1983) *Principles of Fluorescence Spectroscopy*, Plenum Press, New York.
23. Miura, T., and Thomas, G. J., Jr. (1995) in *Subcellular Biochemistry, Volume 24. Proteins: Structure, Function, and Engineering* (Biswas, B. B., and Roy, S., Eds.) pp 55−99, Plenum Press, New York.
24. Siamwiza, M. N., Lord, R. C., Chen, M. C., Takamatsu, T., Harada, I., Matsuura, H., and Shimanouchi, T. (1975) *Biochemistry 14*, 4870−4876.
25. Erfurth, S. C., Kiser, E. J., and Peticolas, W. L. (1972) *Proc. Natl. Acad. Sci. U.S.A. 69*, 938−941.
26. Prescott, B., Steinmetz, W., and Thomas, G. J., Jr. (1984) *Biopolymers 23*, 235−256.
27. Miura, T., and Thomas, G. J., Jr. (1994) *Biochemistry 33*, 7848−7856.
28. Thomas, G. J., Jr., and Tsuboi, M. (1993) *Adv. Biophys. Chem. 3*, 1−70.
29. Nishimura, Y., Tsuboi, M., Kato, S., and Morokuma, K. (1985) *Bull. Chem. Soc. Jpn. 58*, 638−643.
30. Duguid, J., Bloomfield, V., Benevides, J. M., and Thomas, G. J., Jr. (1993) *Biophys. J. 65*, 1916−1928.
31. Laporte, L., and Thomas, G. J., Jr. (1997) Submitted for publication.

32. Miura, T., Benevides, J. M., and Thomas, G. J., Jr. (1995) *J. Mol. Biol. 248*, 233−238.
33. Benevides, J. M., Weiss, M. A., and Thomas, G. J., Jr. (1991) *Biochemistry 30*, 5955−5963.
34. Benevides, J. M., Kukolj, G., Autexier, C., Aubrey, K. L., DuBow, M. S., and Thomas, G. J., Jr. (1994) *Biochemistry 33*, 10701−10710.
35. Thomas, G. J., Jr., and Benevides, J. M. (1985) *Biopolymers 24*, 1101−1105.
36. Takeuchi, H., Watanabe, N., and Harada, I. (1986) *Spectrochim. Acta 44A*, 749−761.
37. Miura, T., Takeuchi, H., and Harada, I. (1991) *Biochemistry 30*, 6074−6080.
38. Kelly, R. C., and von Hippel, P. H. (1976) *J. Biol. Chem. 251*, 7229−7239.
39. Gupta, G., Garcia, A. E., Guo, Q., Lu, M., and Kallenbach, N. (1993) *Biochemistry 32*, 3596−3603.

BI972400D